Degrafting reaction of polymer brushes: the determining role of molecular weight and grafting density

Riccardo Chiarcos[a], Diego Antonioli[a], Luca Gabutti[a], Elo Marsengo[a], Michele Perego[b] and Michele Laus[a]

[a]Department of Science and Technological Innovation (DISIT), Università del Piemonte Orientale (UPO), Alessandria 15121, Italy
[b]Institute for Microelectronics and Microsystems (IMM), National Research Council of Italy (CNR), Agrate Brianza 20864, Italy

riccardo.chiarcos@uniupo.it

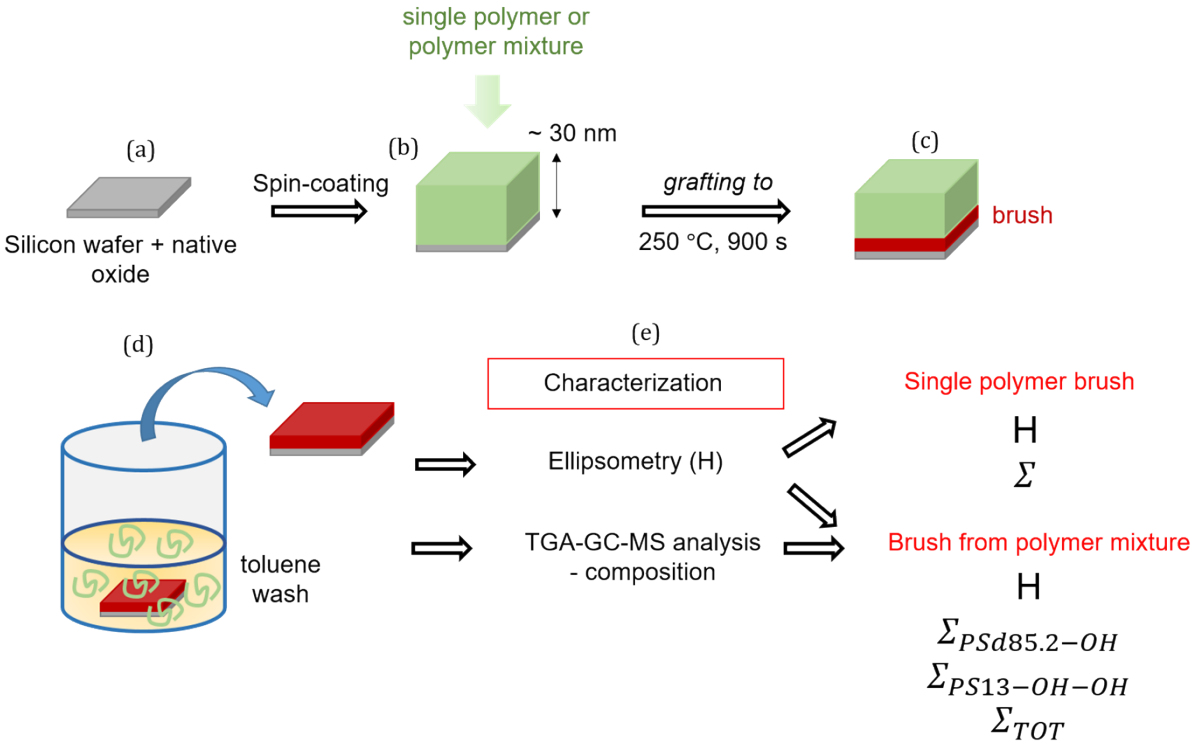

Figure S1. Workflow of the grafting to process.

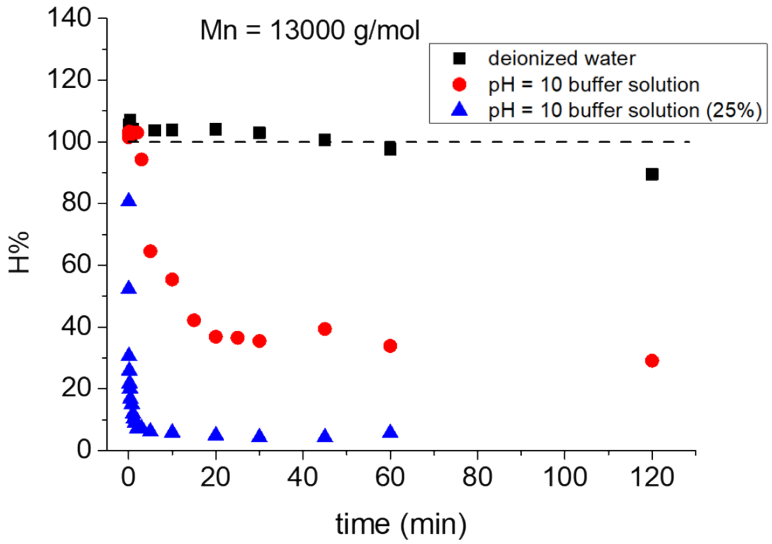

Figure S2. Residual percentage (H%) of the brush thickness after exposure to deionized water (black dots), pH = 10 buffer solution (red dots) and pH = 10 buffer solution (25%) / THF (75%) mixture. These three different conditions were tested on polymer brushes obtained with PS13-OH.

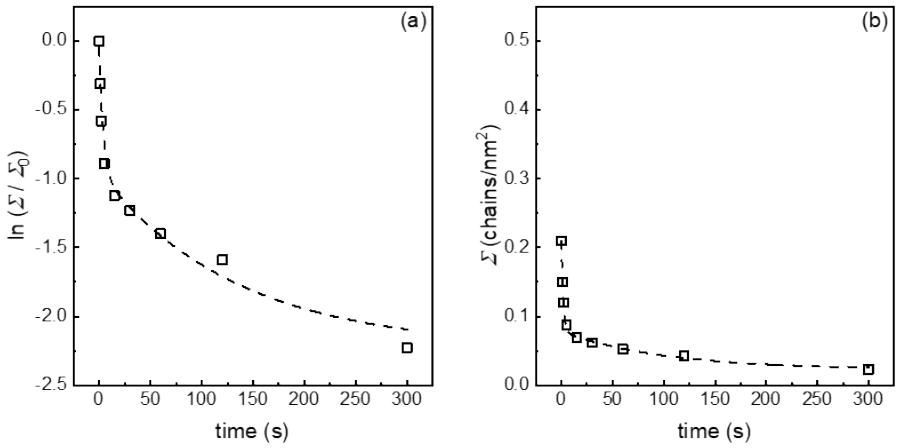

Figure S3. Ln(Σ/Σ_0) vs degrafting time **(a)** and Σ vs degrafting time **(b)** for the polymer brush consisting of PS43.2-OH. The experimental data are reported as black dots, while the data fitting was performed with the software Origin using a double factor exponential decay function.

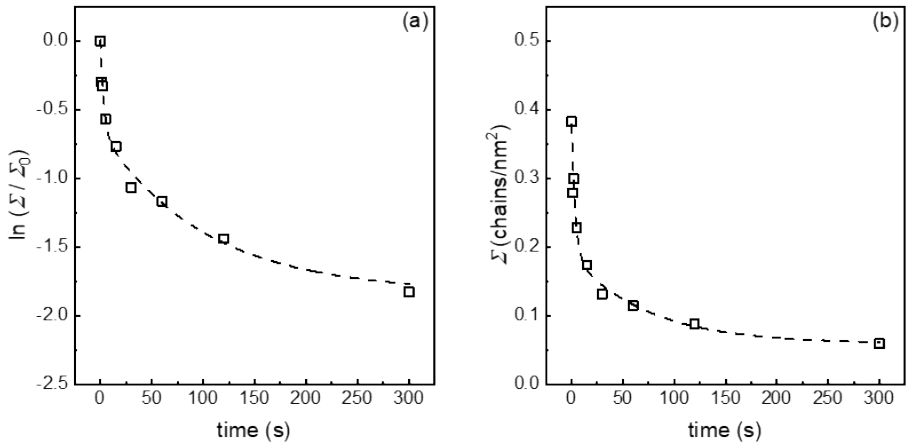

Figure S4. Ln(Σ/Σ_0) vs degrafting time **(a)** and Σ vs degrafting time **(b)** for the polymer brush consisting of PS13-OH. The experimental data are reported as black dots, while the data fitting was performed with the software Origin using a double factor exponential decay function.

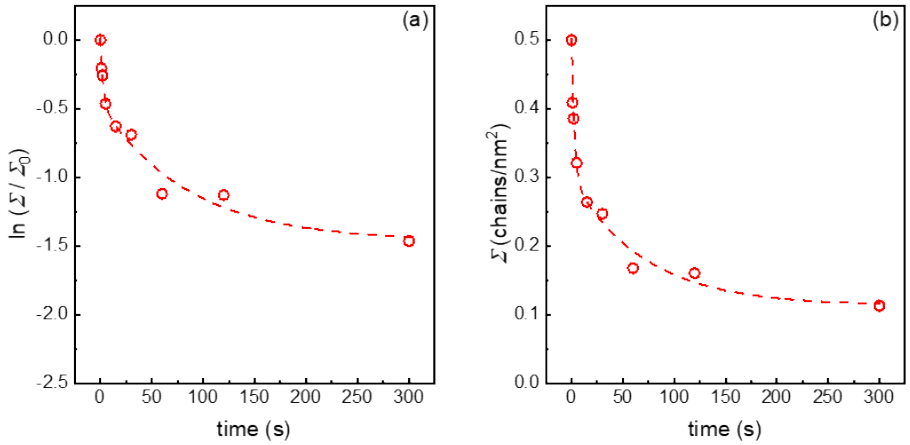

Figure S5. Ln(Σ/Σ_0) vs degrafting time **(a)** and Σ vs degrafting time **(b)** for the polymer brush consisting of PS_{d8}5.2-OH. The experimental data are reported as red dots, while the data fitting was performed with the software Origin using a double factor exponential decay function.

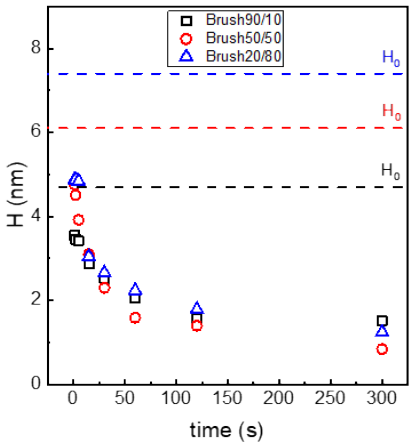

Figure S6. H values as a function of the degrafting time for the brushes Brush90 (black dots), Brush50 (red dots) and Brush20 (blue dots). The values of H_0, relative to the brushes before degrafting, are also included as dotted lines.

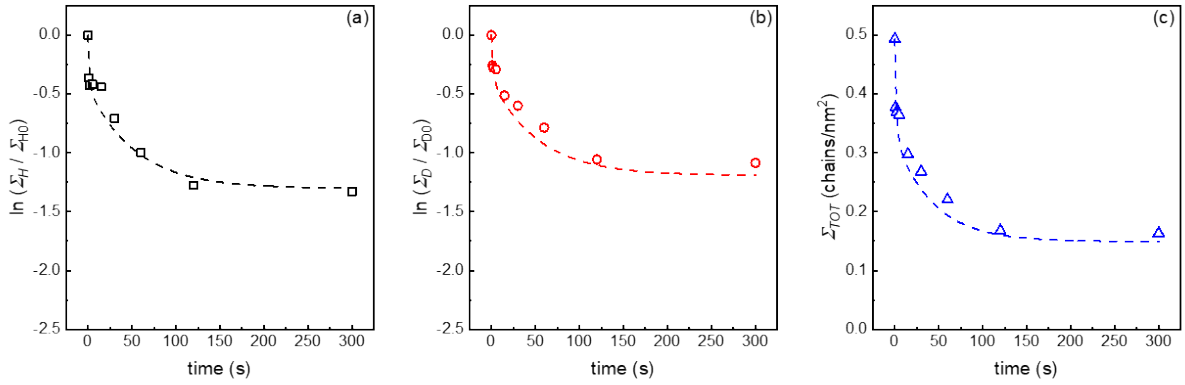

Figure S7. $Ln(\Sigma_H/\Sigma_{H,0})$ **(a)**, $Ln(\Sigma_D/\Sigma_{D,0})$ **(b)** and Σ_{TOT} **(c)** vs degrafting time for Brush90. The experimental data are reported as black, red and blue dots, respectively, while the data fitting was performed with the software Origin using a double factor exponential decay function.

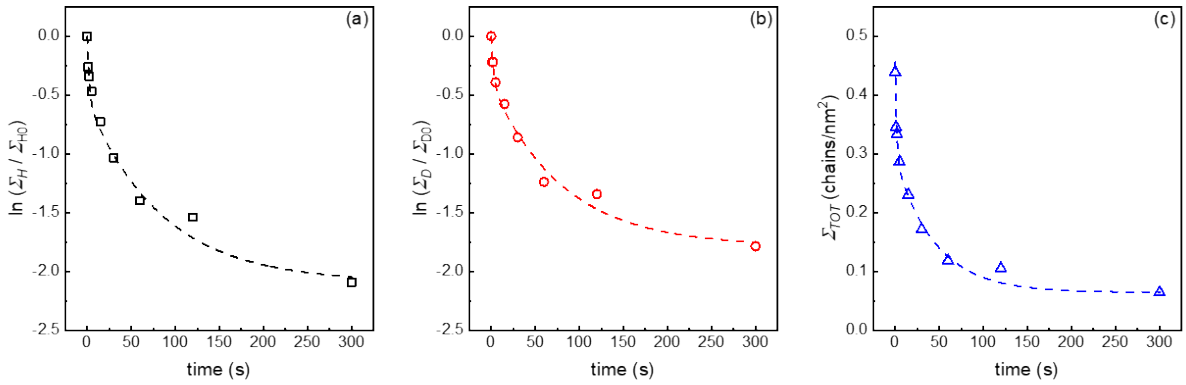

Figure S8. $Ln(\Sigma_H/\Sigma_{H,0})$ **(a)**, $Ln(\Sigma_D/\Sigma_{D,0})$ **(b)** and Σ_{TOT} **(c)** vs degrafting time for Brush50. The experimental data are reported as black, red and blue dots, respectively, while the data fitting was performed with the software Origin using a double factor exponential decay function.

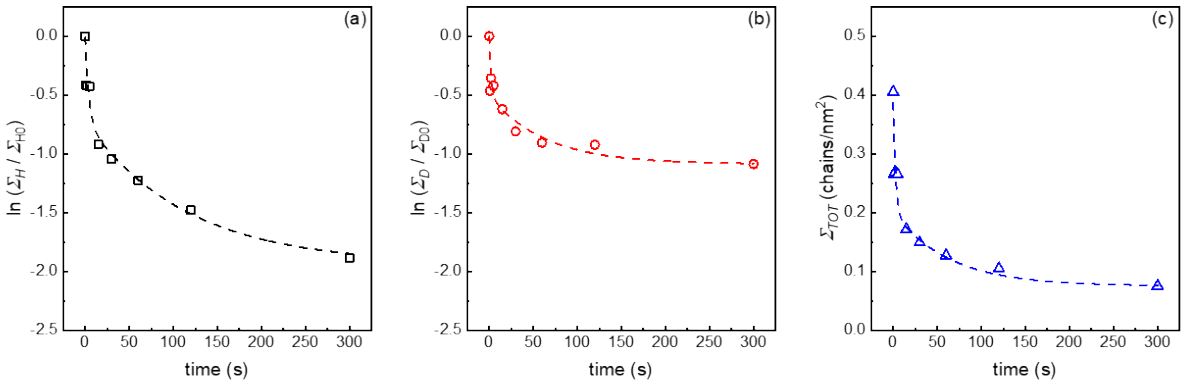

Figure S9. $Ln(\Sigma_H/\Sigma_{H,0})$ **(a)**, $Ln(\Sigma_D/\Sigma_{D,0})$ **(b)** and Σ_{TOT} **(c)** vs degrafting time for Brush20. The experimental data are reported as black, red and blue dots, respectively, while the data fitting was performed with the software Origin using a double factor exponential decay function.

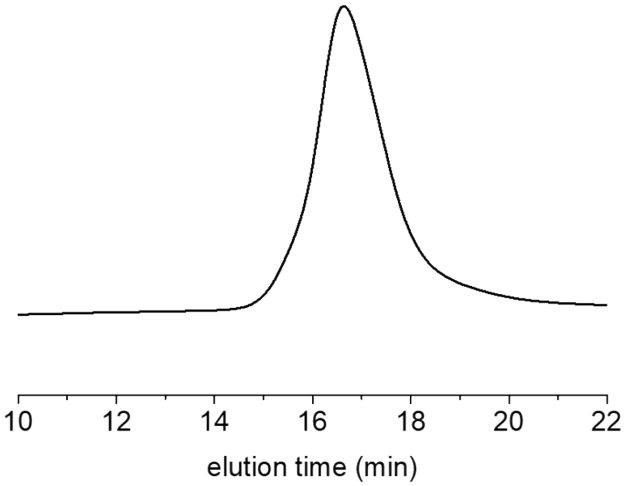

Figure S10. SEC chromatograph of the PS43.2-OH sample.